Light nuclei production in HIC: from coalescence model to kinetic approach

Che-Ming Ko
Texas A&M University

- Introduction
  - Light nuclei as a probe to EOS and phase diagram of QCD matter
- The coalescence model
  - History and present status
  - Comparison to thermal model
- The kinetic approach
  - Schematic vs dynamic
  - Comparison to coalescence model
- Summary

VOLUME 43, NUMBER 20 PHYSICAL REVIEW LETTERS 12 NOVEMBER 1979

Evidence for a Soft Nuclear-Matter Equation of State

Philip J. Siemens[(a)] and Joseph I. Kapusta
Lawrence Berkeley Laboratory, University of California, Berkeley, California 94720
(Received 3 August 1979)

The entropy of the fireball formed in central collisions of heavy nuclei at center-of-mass kinetic energies of a few hundred MeV per nucleon is estimated from the ratio of deuterons to protons at large transverse momentum. The observed paucity of deuterons suggests that strong attractive forces are present in hot, dense nuclear matter, or that degrees of freedom beyond the nucleon and pion may already be realized at an excitation energy of 100 MeV per baryon.

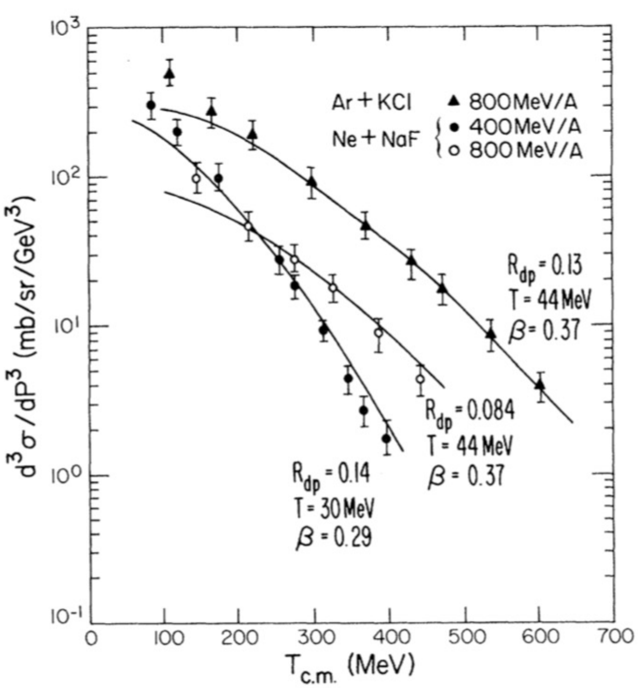

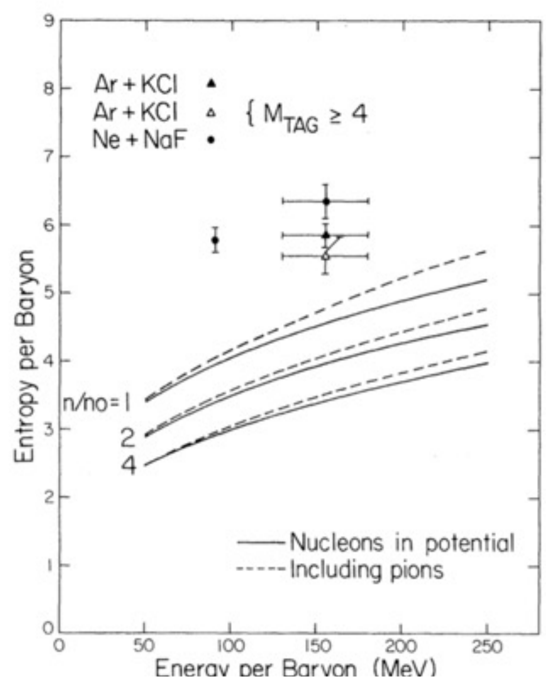

Entropy per nucleon

$$\frac{S}{N} \approx 3.95 - \ln \frac{N_d}{N_p}$$

Isobaric yield ratio of t/He

Chen, Li &Ko, PRC 68, 017601 (2003); NPA 729, 809 (2003)

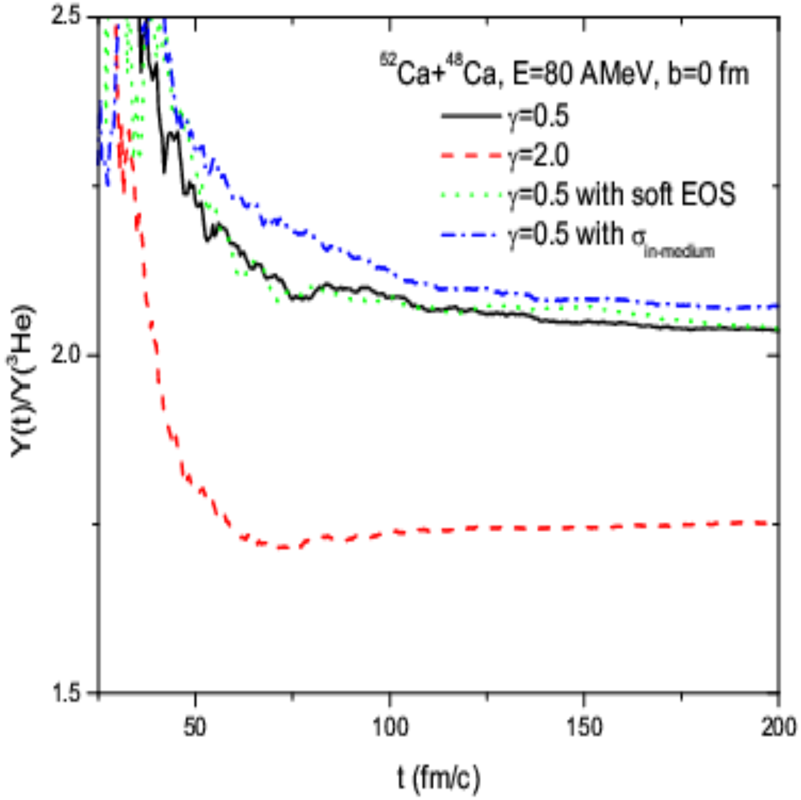

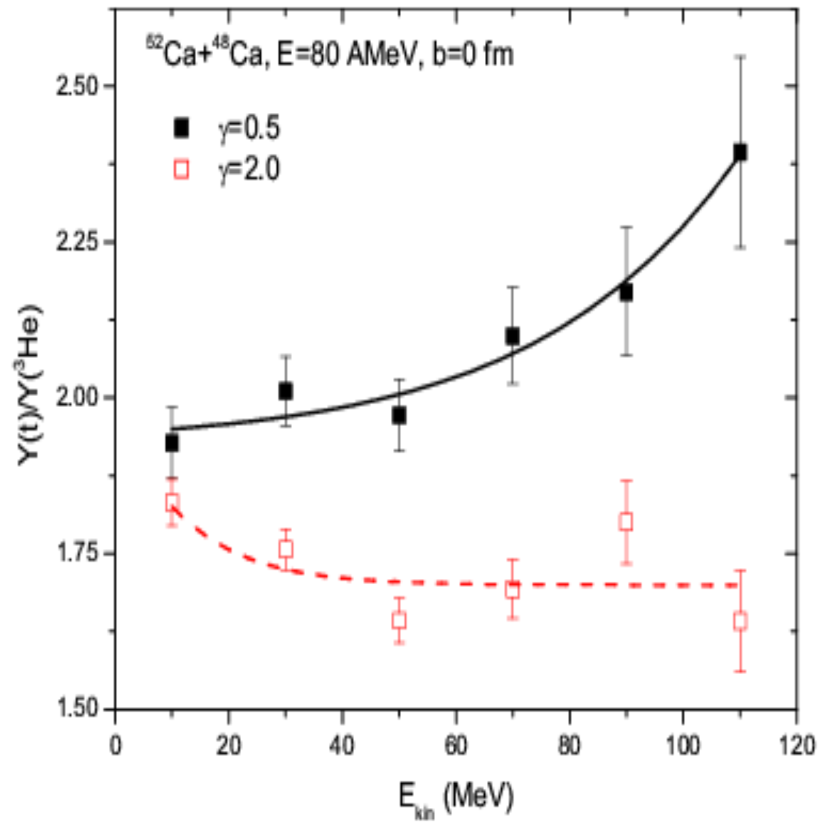

- t and He are produced using the coalescence model
- Stiffer symmetry energy gives smaller t/He ratio
- t/He ratio increases (stiff symmetry energy) but slightly decreases (soft symmetry energy) with their kinetic energies

Yield ratio of $N_t N_p / N_d^2$ in Au+Au collisions at RHIC

STAR Collaboration, arXiv:2209.08058 [nucl-ex]

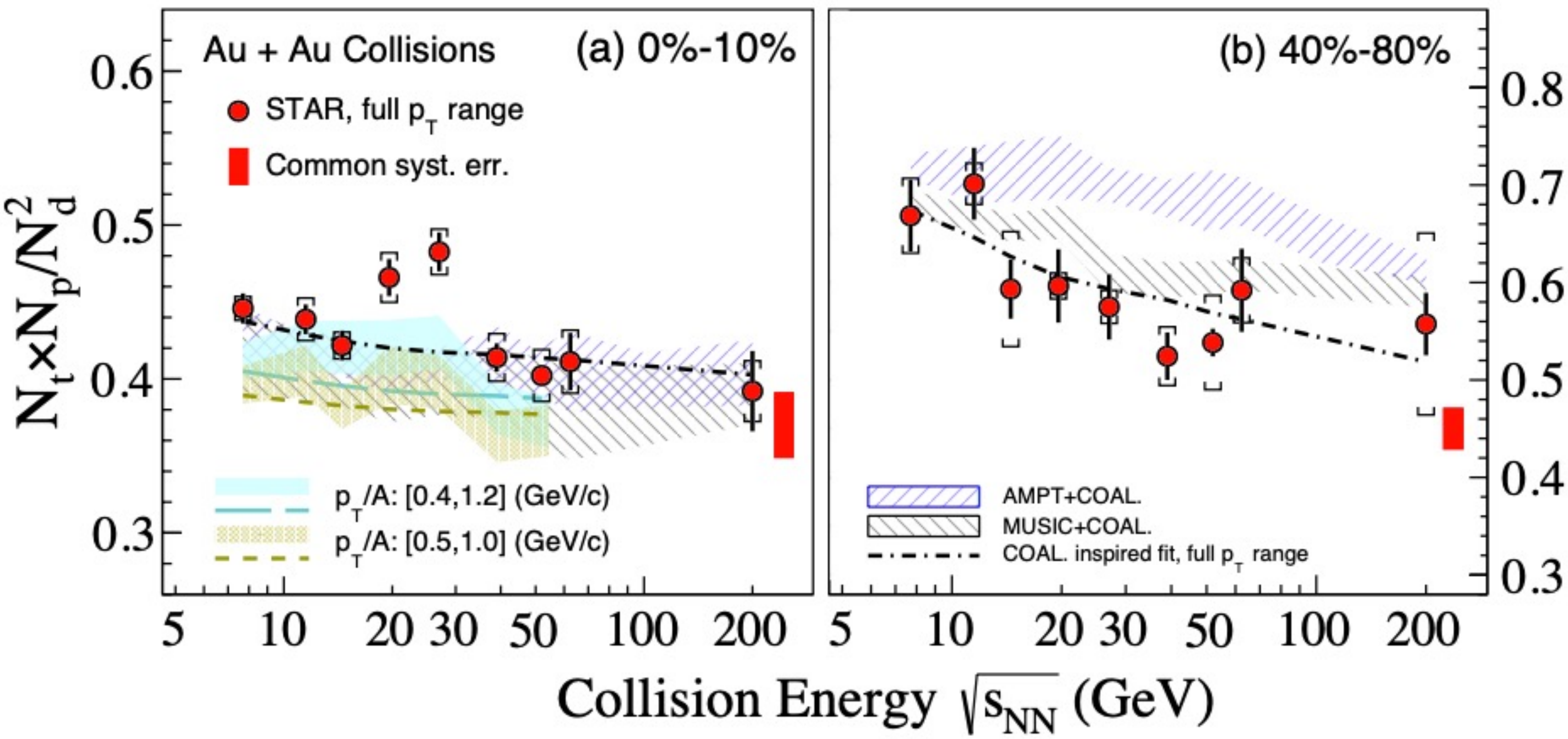

- Enhanced yield ratio of $N_t N_p / N_d^2$ at $\sqrt{s_{NN}} \approx 25$ GeV in central Au+Au collisions, compared to non-central collisions.

Beam-energy dependence of $N_t N_p / N_d^2$ from theoretical models

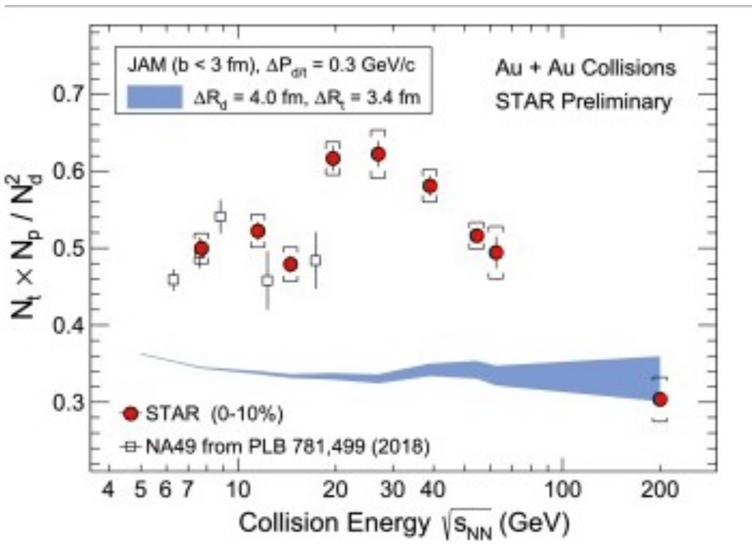

Liu, Zhang, He, Sun, Yu, Luo, PLB 805, 135452 (2020): JAM

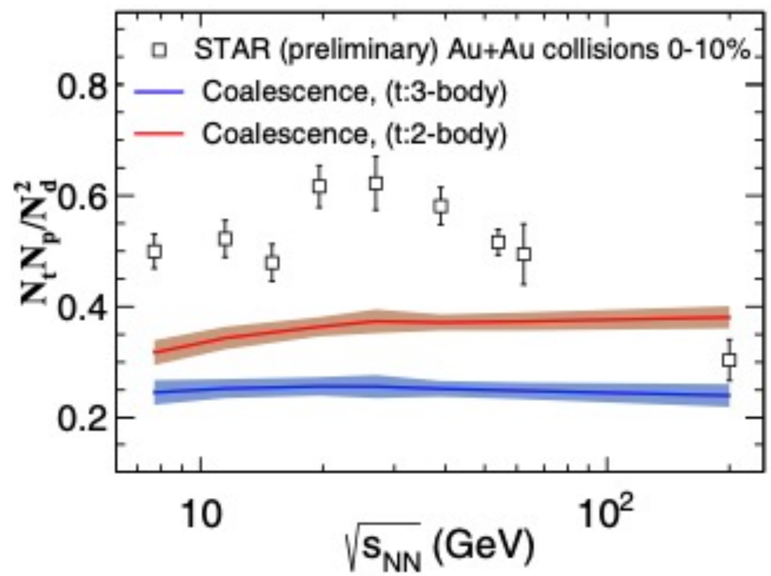

Zhao, Shen, Ko, Liu & Song, PRC 102, 044912 (2020). IEBE+MUSIC+UrQMD

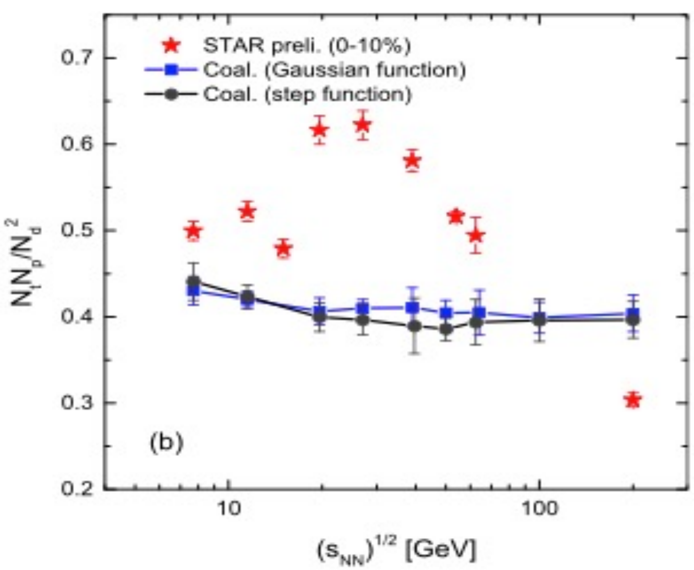

Sun, Ko & Lin, PRC 103, 064909 (2021); AMPT

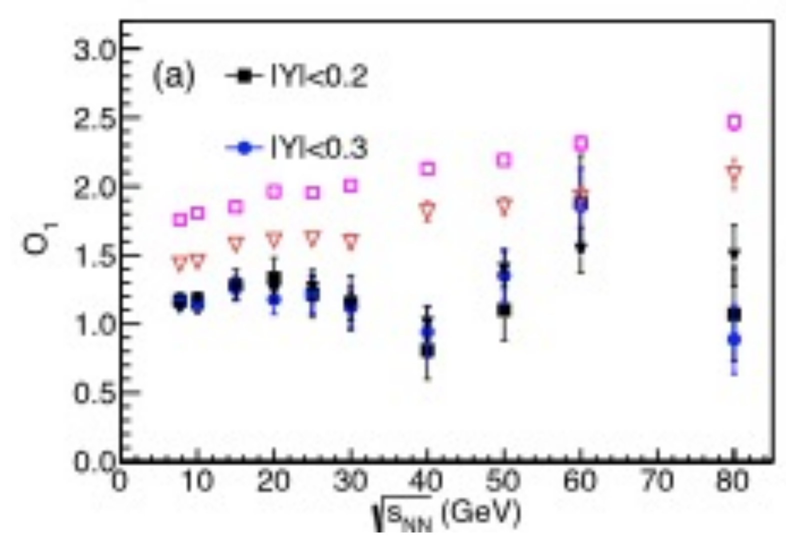

Deng & Ma, PLB 808, 135668 (2020): UrQMD

Quark matter phase diagram in the NJL model

$$\mathcal{L} = \bar\psi(i\gamma^\mu\partial_\mu - \hat m)\psi + G_S\sum_{a=0}^{8}[(\bar\psi\lambda^a\psi)^2 + (\bar\psi i\gamma_5\lambda^a\psi)^2]$$
$$-g_V(\bar\psi\gamma^\mu\psi)^2 - K[\det\bar\psi(1+\gamma_5)\psi + \det\bar\psi(1-\gamma_5)\psi]$$

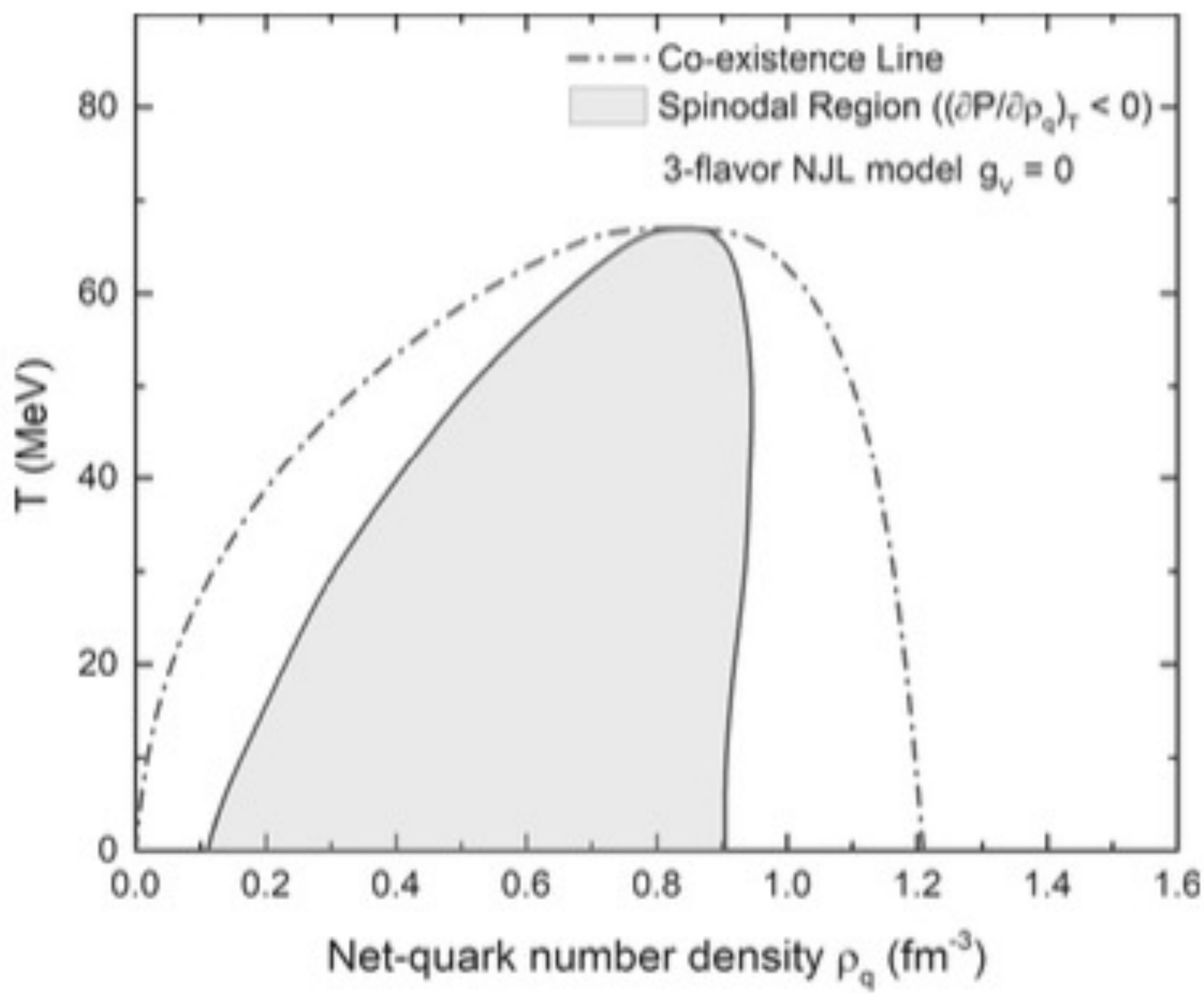

Transport description of quark matter in a box based on NJL

$$\partial_t f + \mathbf{p}/E \cdot \nabla f - \nabla H \cdot \nabla_p f = \mathcal{C}[f]$$

Feng & Ko, PRC 93, 035205 (16); 95, 055203 (17)

C[f] includes quark elastic scattering with cross section of 3 mb

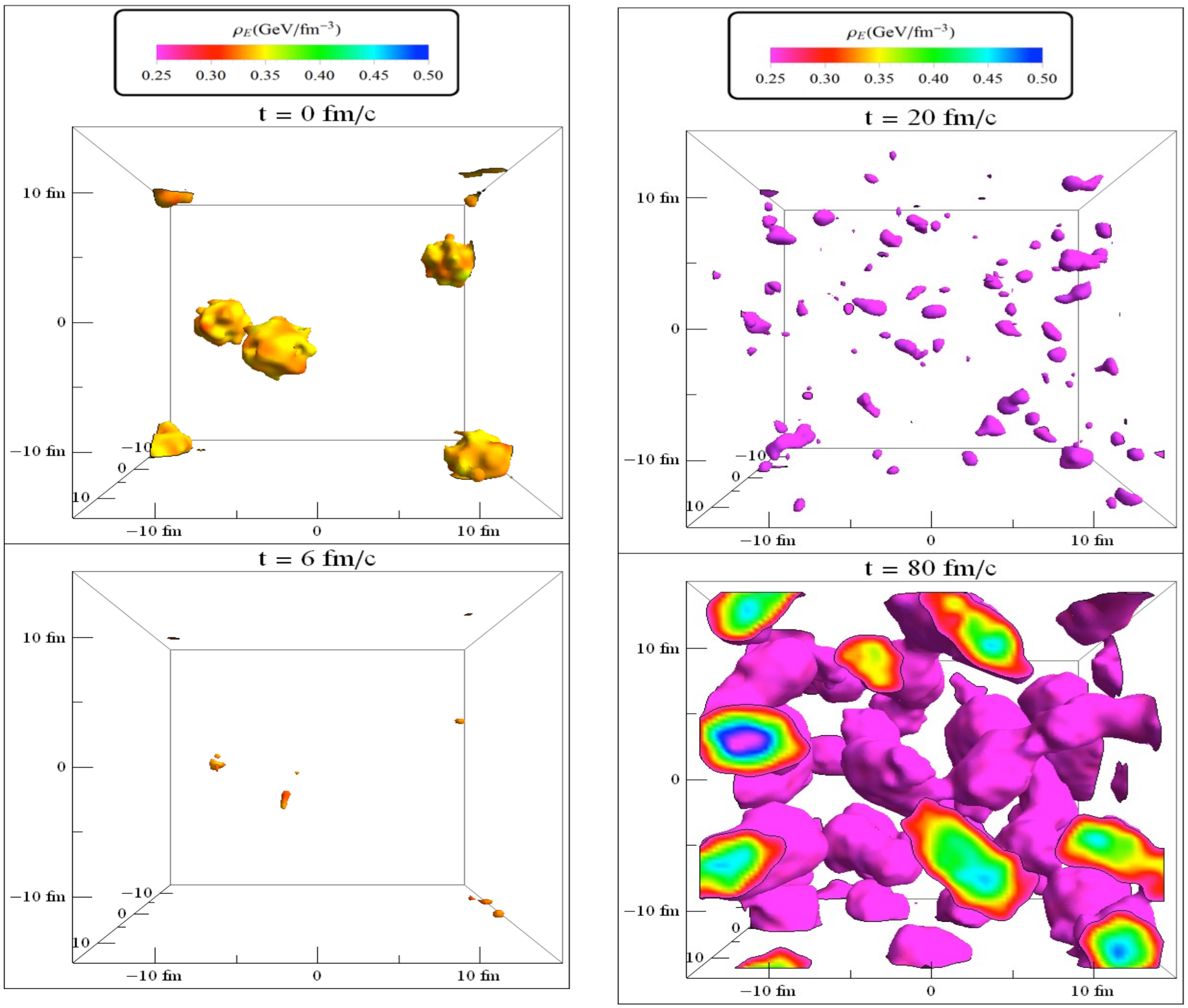

- Left: $n_q = 0.4/fm^3$, T = 100 MeV; outside spinodal region
- Right: $n_q = 0.4/fm^3$, T = 20 Mev, inside spinodal region; large density fluctuations appear due to growth of unstable modes
- Colored regions correspond to $N_q > 0.6/fm^3$

$N_t N_p / N_d^2$ Enhancement due to chiral first-order trasnsition

Sun, Ko, Li, Xu & Chen, EPJA 57, 31 (2021)

AMPT with blast-wave initial conditions with T= 70 MeV and net quark density 1.5/fm^3 and NJL based parton transport model

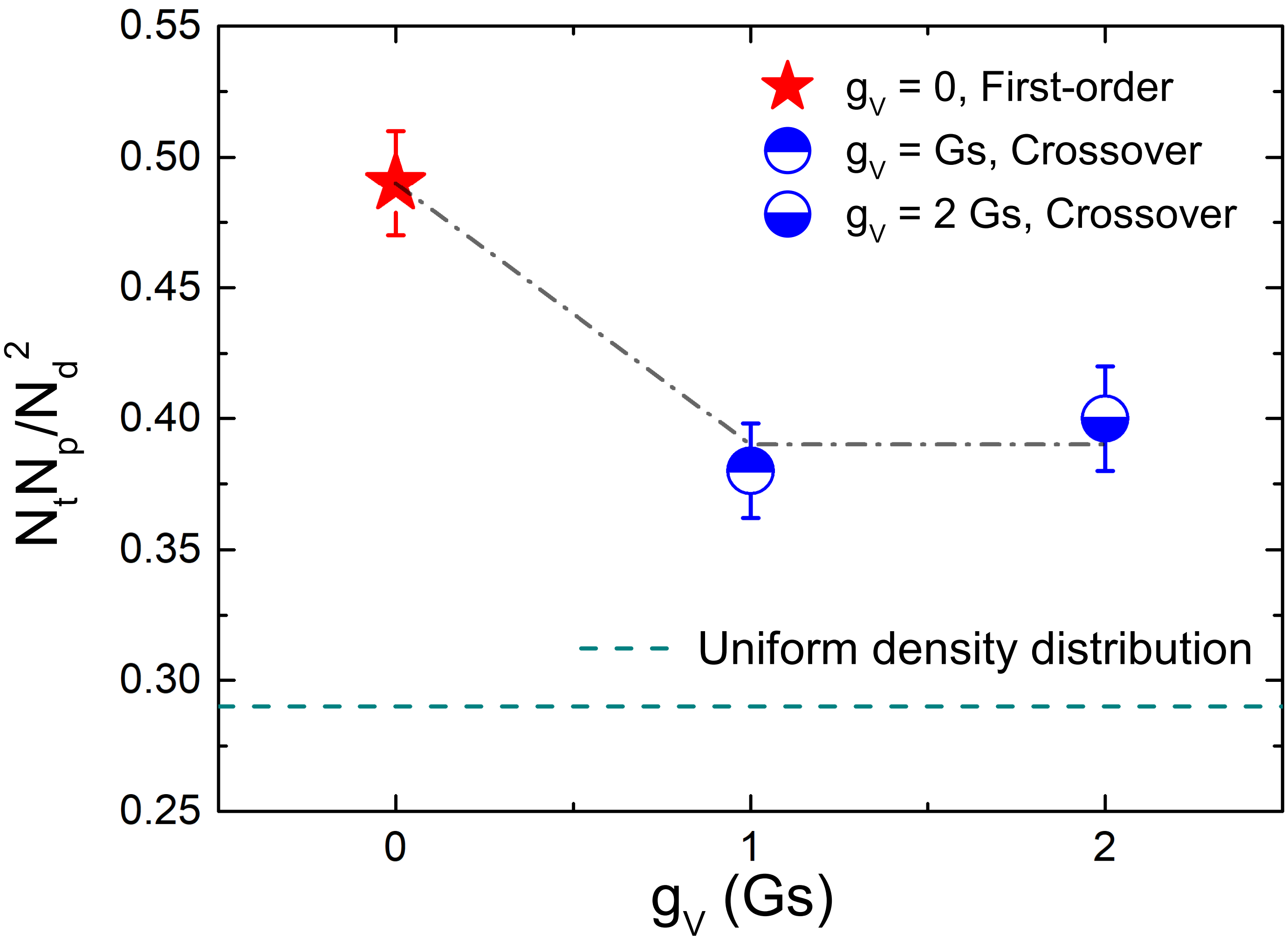

The coalescence model

1) Butler and Pearson, PR 129, 836 (1963): Two nucleons coalescence into a deuteron with the nuclear matter acting as a catalyzer. In second-order perturbation theory,

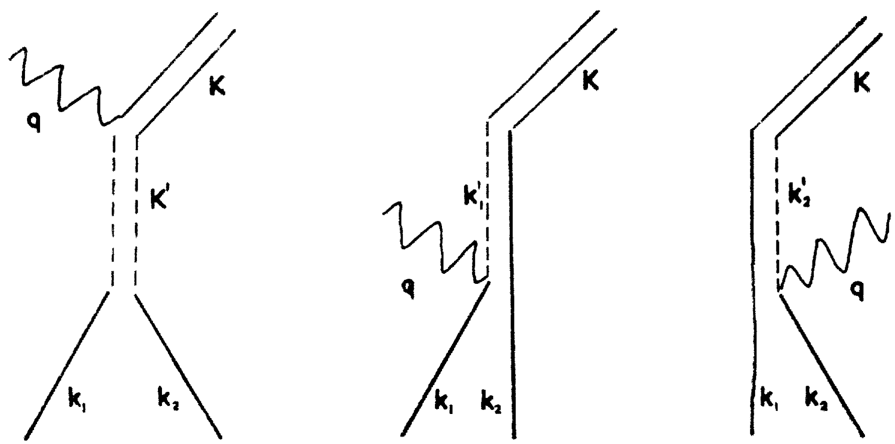

$$N_d(\mathbf{K}) \propto [N_p(\mathbf{K}/2)]^2$$

2) Schwalzschild and Zupancic, PR 129, 854 (1963): The deuteron-to-proton ratio is governed by the probability of finding a neutron within a small sphere of radius ρ around the proton in momentum space

$$dN_d(K)/dN_p(K) \propto \frac{4\pi\rho^3}{3}$$

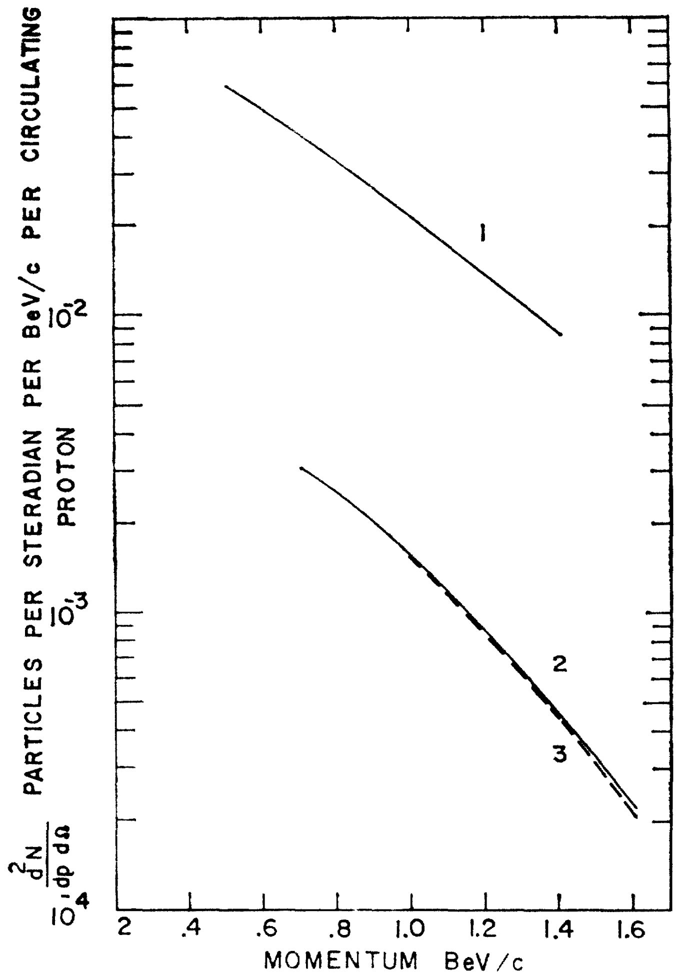

FIG. 3. A comparison of the observed and calculated momentum distributions for deuterons produced from a Be target at an angle of 45° in the laboratory system by protons with incident energy 30 BeV. Curves 2 and 3 are the observed and the calculated deuteron distribution (34). Curve 1 is the experimental distribution of cascade protons used to calculate (34). The experimental data are those of Fitch *et al.* (reference 3).

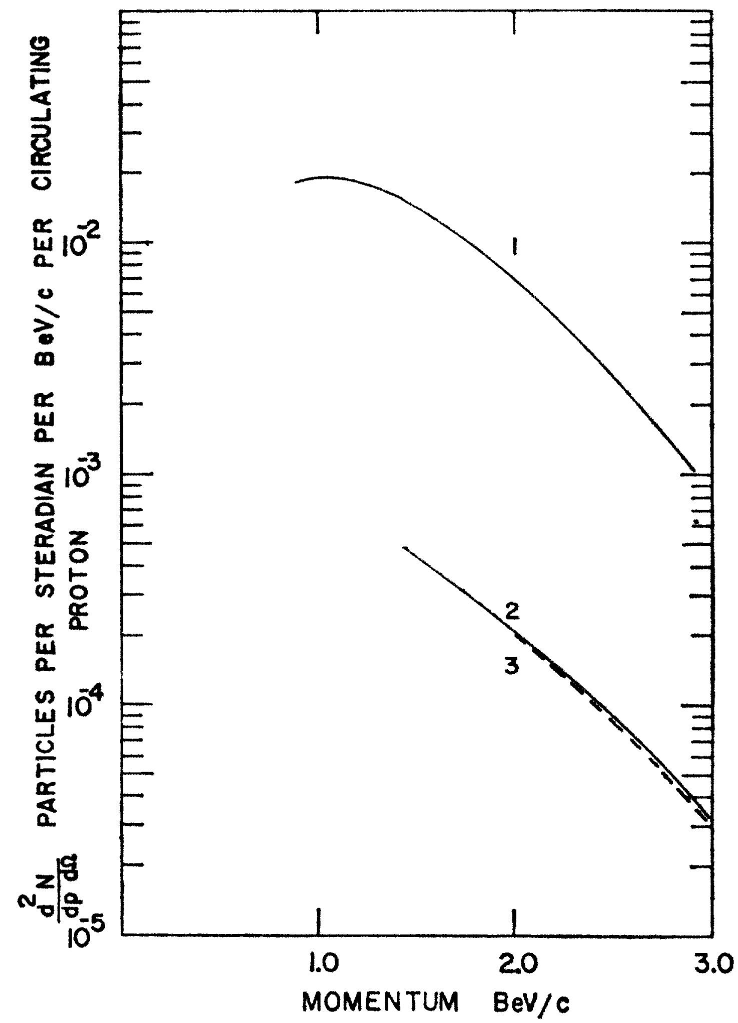

FIG. 4. As in Fig. 3, the deuterons are produced from a Be target at an angle of 30° in the laboratory system by protons with incident energy 30 BeV. The curves are labeled as in Fig. 3, and the experimental results are those of Schwarzschild and Županči̇č (reference 6).

Coalescence production of light nuclei at Bevalac

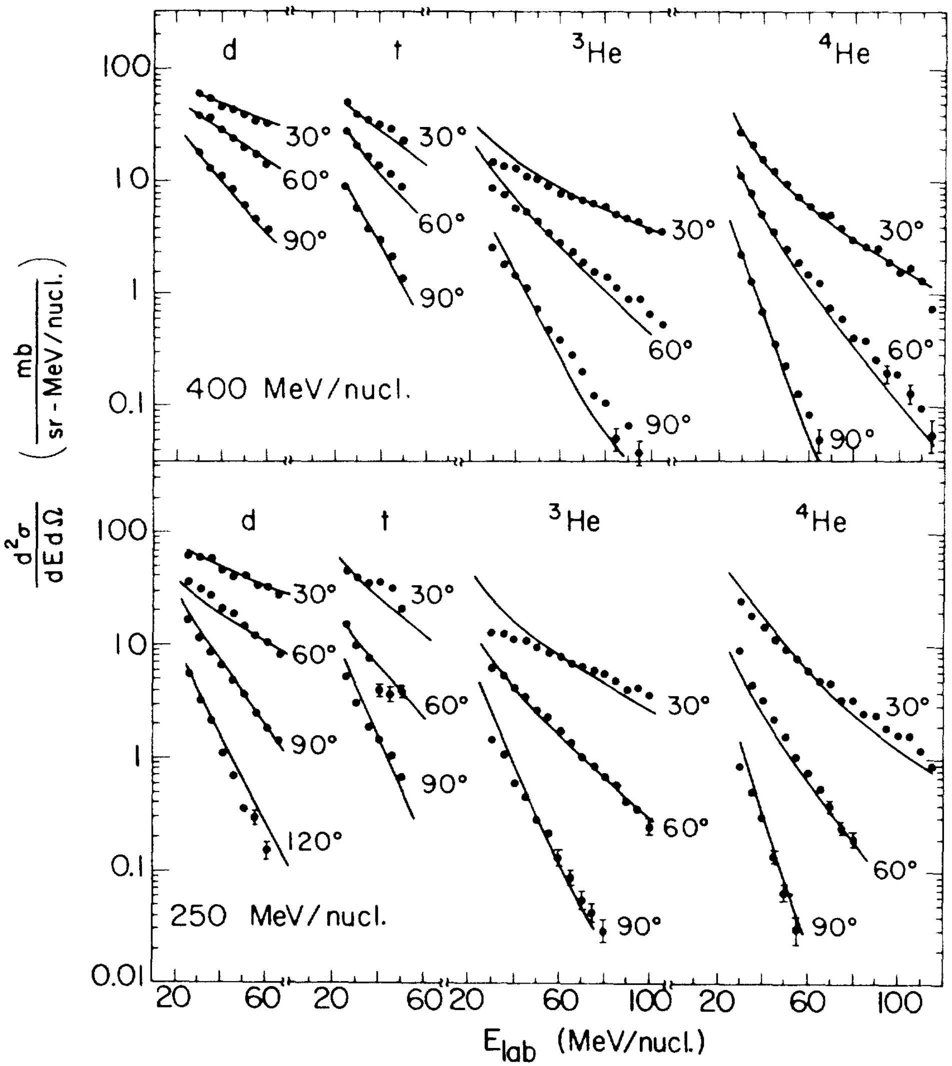

FIG. 3. Experimental points and calculated lines for the double-differential cross sections of fragments from the irradiation of uranium by ^{20}Ne ions at 250 and 400 MeV/nucleon.

Gutbrod et al., PRL 37, 667 (1976)

$$E_A \frac{d^3 N_A}{dp_A^3} = B_A \left(E_p \frac{d^3 N_p}{dp_p^3} \right)^A$$

$$B_A = \left(\frac{4\pi}{3} p_0^3 \right)^{A-1} \frac{M}{m^A}, \; p_A = A p_p$$

Coalescence radius p_0 (MeV)

Nuclei	250	400
d	126	129
t	140	129
^{3}He	135	129
^{4}He	157	142

Butler & Peterson, PR 129, 836 (1963)
Schwalzchild & Zupancic, PR 129, 854 (1963)

Coalescence model as an impulse approximation

Wave functions for initial |i>=|1,2> and final |f>=|3> states

$$\langle \mathbf{r}_1, \mathbf{r}_2 | i \rangle = \phi_1(\mathbf{r}_1)\phi_2(\mathbf{r}_2)$$

$$\langle \mathbf{r}_1, \mathbf{r}_2 | f \rangle = \frac{1}{\sqrt{V}} e^{i\mathbf{K}\cdot(\mathbf{r}_1+\mathbf{r}_2)/2} \Phi(\mathbf{r}_1 - \mathbf{r}_2)$$

Probability for 1+2 -> 3 $\quad \mathcal{P} = |\langle f | i \rangle|^2$

Probability for particle 1 of momentum $\mathbf{k}_1$ and particle 2 of momentum $\mathbf{k}_2$ to coalescence to cluster 3 with momentum $\mathbf{K}$

$$\frac{dN}{d^3\mathbf{K}} = g \int d^3\mathbf{x}_1 d^3\mathbf{k}_1 d^3\mathbf{x}_2 d^3\mathbf{k}_2 W_1(\mathbf{x}_1, \mathbf{k}_1) W_2(\mathbf{x}_2, \mathbf{k}_2)$$

$$\times W(\mathbf{y}, \mathbf{k}) \delta^{(3)}(\mathbf{K} - \mathbf{k}_1 - \mathbf{k}_2), \qquad \mathbf{y} = \mathbf{x}_1 - \mathbf{x}_2, \quad \mathbf{k} = \frac{\mathbf{k}_1 - \mathbf{k}_2}{2}$$

Wigner functions $\quad W(\mathbf{x}, \mathbf{k}) = \int d^3\mathbf{y} \phi^* \left(\mathbf{x} - \frac{\mathbf{y}}{2}\right) \phi \left(\mathbf{x} + \frac{\mathbf{y}}{2}\right) e^{-i\mathbf{k}\cdot\mathbf{y}}$

For a system of particles 1 and 2 with phase-space distributions $f_i(\mathbf{x}_i,\mathbf{k}_i)$ normalized to $\int d^3\mathbf{x_i} d^3\mathbf{k}_i f_i(\mathbf{x}_i,\mathbf{k}_i) = N_i$, the number of particle 3 produced from coalescence of N_1 of particle 1 and N_2 of particle 2

$$\frac{dN}{d^3\mathbf{K}} \approx g \int d^3\mathbf{x}_1 d^3\mathbf{k}_1 d^3\mathbf{x}_2 d^3\mathbf{k}_2 f_1(\mathbf{x}_1,\mathbf{k}_1) f_2(\mathbf{x}_2,\mathbf{k}_2) \times \overline{W}(\mathbf{y},\mathbf{k})\delta^{(3)}(\mathbf{K}-\mathbf{k}_1-\mathbf{k}_2)$$

$$\overline{W}(\mathbf{y},\mathbf{k}) = \int \frac{d^3\mathbf{x}_1' d^3\mathbf{k}_1'}{(2\pi)^3} \frac{d^3\mathbf{x}_2' d^3\mathbf{k}_2'}{(2\pi)^3} W_1(\mathbf{x}_1',\mathbf{k}_1') W_2(\mathbf{x}_2',\mathbf{k}_2') W(\mathbf{y}',\mathbf{k}')$$

Wigner function $W_i(\mathbf{x}_i',\mathbf{k}_i')$ centers around $\mathbf{x}_i$ and $\mathbf{k}_i$

$$g = \frac{2J+1}{(2J_1+1)(2J_2+1)}$$

Statistical factor for two particles of spin J_1 and J_2 to form a particle of spin J

The above formula can be straightforwardly generalized to multi-particle coalescence, but is usually used by taking particle Wigner functions as delta functions in space and momentum.

Gyulassy, Frankel, and Remler, NPA 402, 596 (1983): Generalized coalescence model using nucleon Wigner functions that are delta functions in space and momentum, i.e., evaluating

$$\overline{W}(\mathbf{y},\mathbf{k}) = \int \frac{d^3\mathbf{x}_1' d^3\mathbf{k}_1'}{(2\pi)^3} \frac{d^3\mathbf{x}_2' d^3\mathbf{k}_2'}{(2\pi)^3} W_1(\mathbf{x}_1',\mathbf{k}_1') W_2(\mathbf{x}_2',\mathbf{k}_2') W(\mathbf{y}',\mathbf{k}')$$

with $\quad W_i(\mathbf{x}_i',\mathbf{k}_i') = (2\pi)^3 \delta^3(\mathbf{x}_i' - \mathbf{x}_i)\delta^3(\mathbf{k}_i' - \mathbf{k}_i)$

$$\rightarrow \frac{dN}{d^3\mathbf{K}} \approx g \int d^3\mathbf{x}_1 d^3\mathbf{k}_1 d^3\mathbf{x}_2 d^3\mathbf{k}_2 f_1(\mathbf{x}_1,\mathbf{k}_1) f_2(\mathbf{x}_2,\mathbf{k}_2)$$
$$\times \quad W(\mathbf{y},\mathbf{k})\delta^{(3)}(\mathbf{K} - \mathbf{k}_1 - \mathbf{k}_2)$$

It is later called by Kahana et al. the standard Wigner calculation in contrast to the general one which they called the quantum Wigner calculation.

Coalescence production of light nuclei at AGS

Kahana et al., PRC 54, 388 (1996)

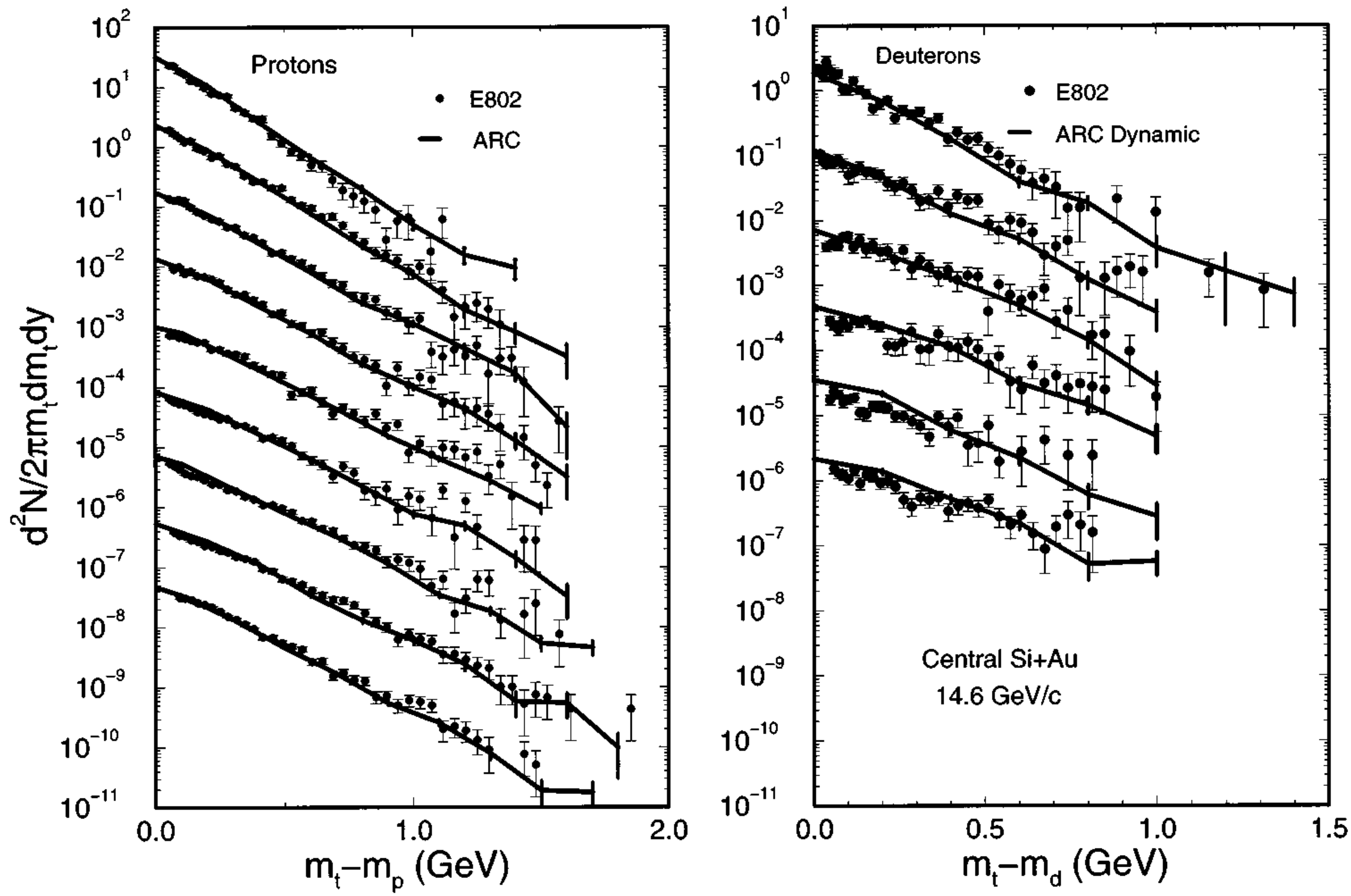

PHYSICAL REVIEW C **98**, 054905 (2018)

Spectra and flow of light nuclei in relativistic heavy ion collisions at energies available at the BNL Relativistic Heavy Ion Collider and at the CERN Large Hadron Collider

Wenbin Zhao,[1,2] Lilin Zhu,[3] Hua Zheng,[4,5] Che Ming Ko,[6] and Huichao Song[1,2,7]

IEBE-VISHNU hybrid model with AMPT initial conditions

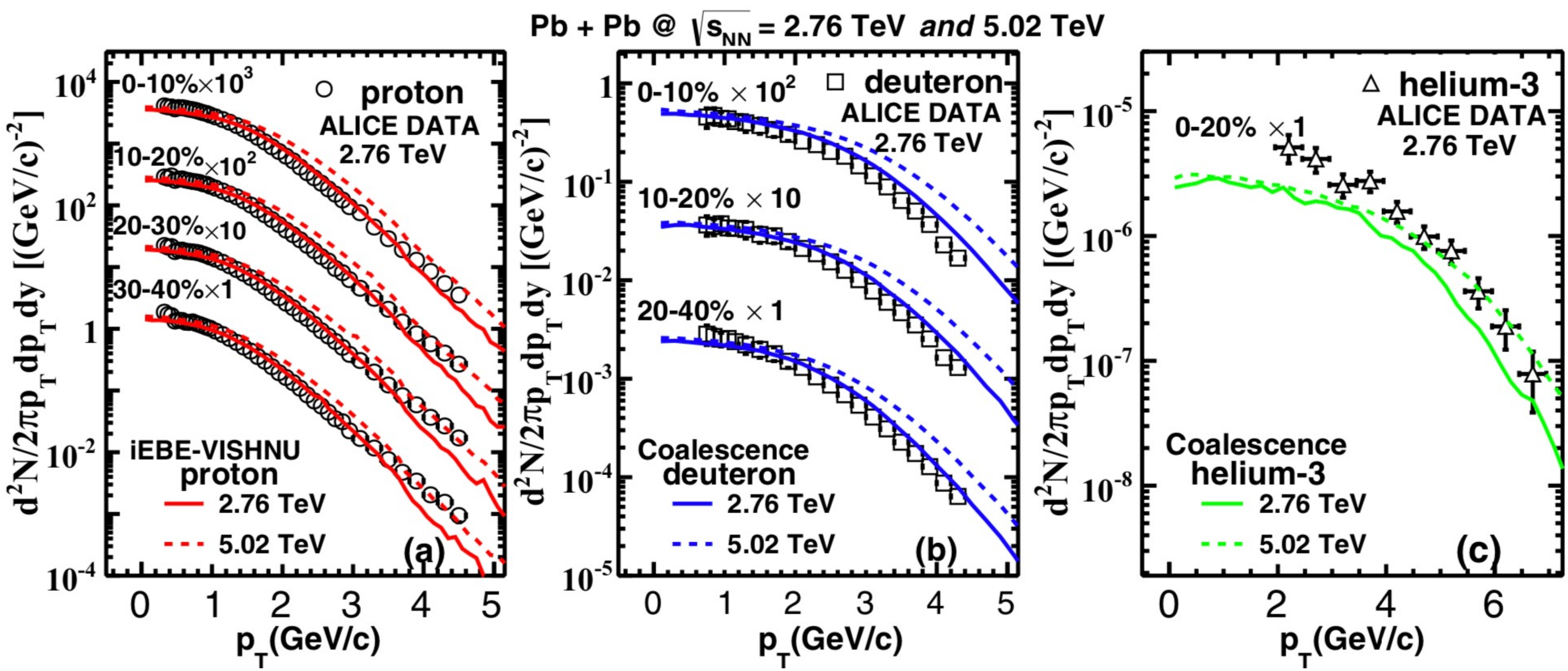

Elliptic flow of deuteron measured by ALICE is also satisfactorily described.

Coalescence vs statistical production of deuteron

With N_p protons and N_n neutrons of temperature T uniformly distributed in V, the deuteron number in coalescence model with Gaussian Wigner function of width parameter σ for deuteron is

$$N_d^{\text{coal}} = \frac{3}{2^{1/2}} \left(\frac{2\pi}{mT} \right)^{3/2} \frac{1}{\left(1 + \frac{1}{mT\sigma^2}\right)^{3/2}} \frac{N_p N_n}{V}$$

while that in the thermal model is

$$N_d^{\text{thermal}} = \frac{3}{2^{1/2}} \left(\frac{2\pi}{mT} \right)^{3/2} \frac{N_p N_n}{V} e^{B_d/T},$$

where B_d is deuteron binding energy. So

$$N_d^{\text{coal}} = N_d^{\text{thermal}} \quad \text{if } T >> B_d \text{ and } mT >> 1/\sigma^2,$$

i.e., temperature of nucleons is much larger than deuteron binding energy and nucleon thermal wavelength is much smaller than deuteron size.

Deuteron production from an extended ART model

Oh & Ko, PRC 76, 054910 (2007); Oh, Lin & Ko, PRC 80, 064902 (2009)

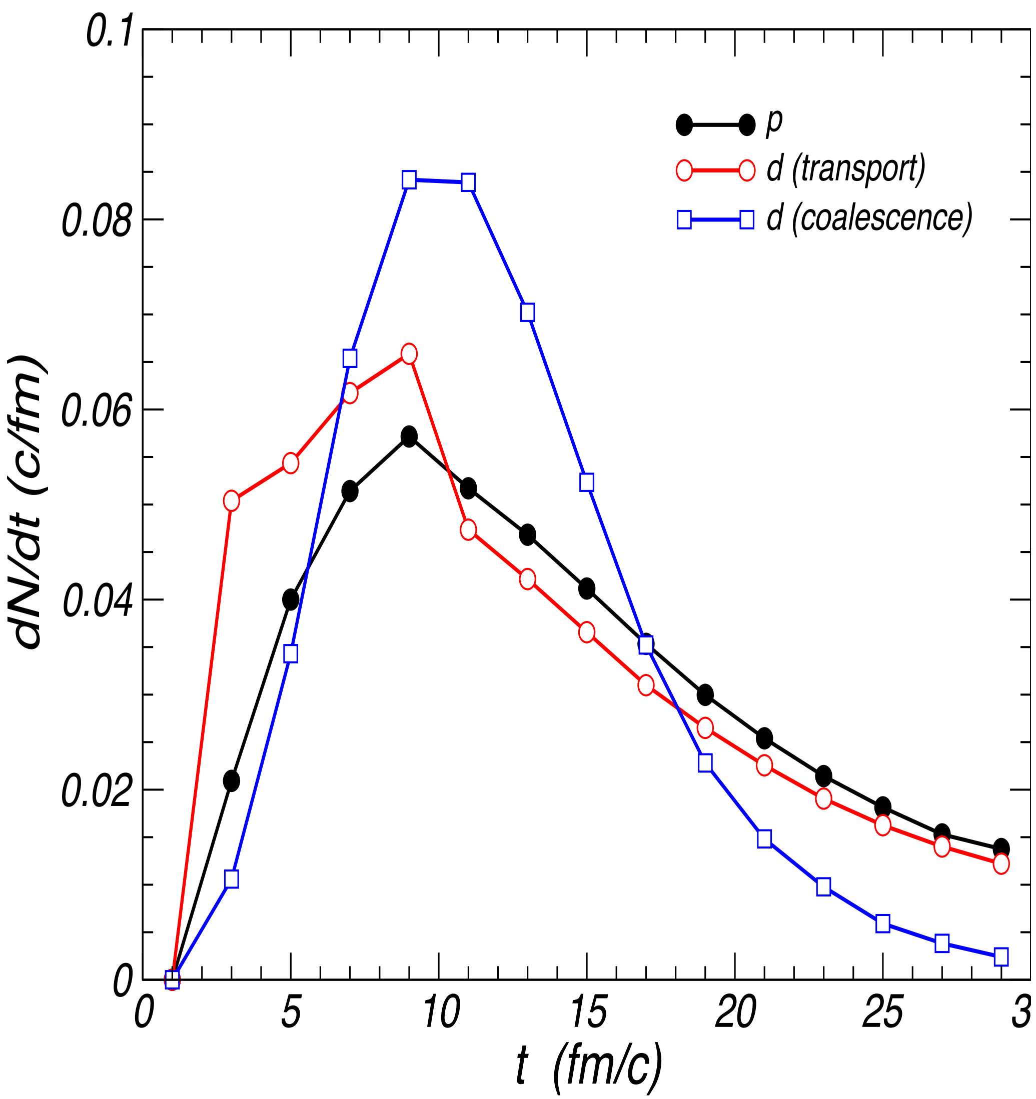

- Include deuteron production ($n+p \rightarrow d+\pi$) and annihilation ($d+\pi \rightarrow n+p$) as well as its elastic scattering
- Similar emission time distributions for protons and deuterons in coalescence model
- Slightly different deuteron emission time distribution in transport and coalescence models

Time evolution of proton and deuteron numbers

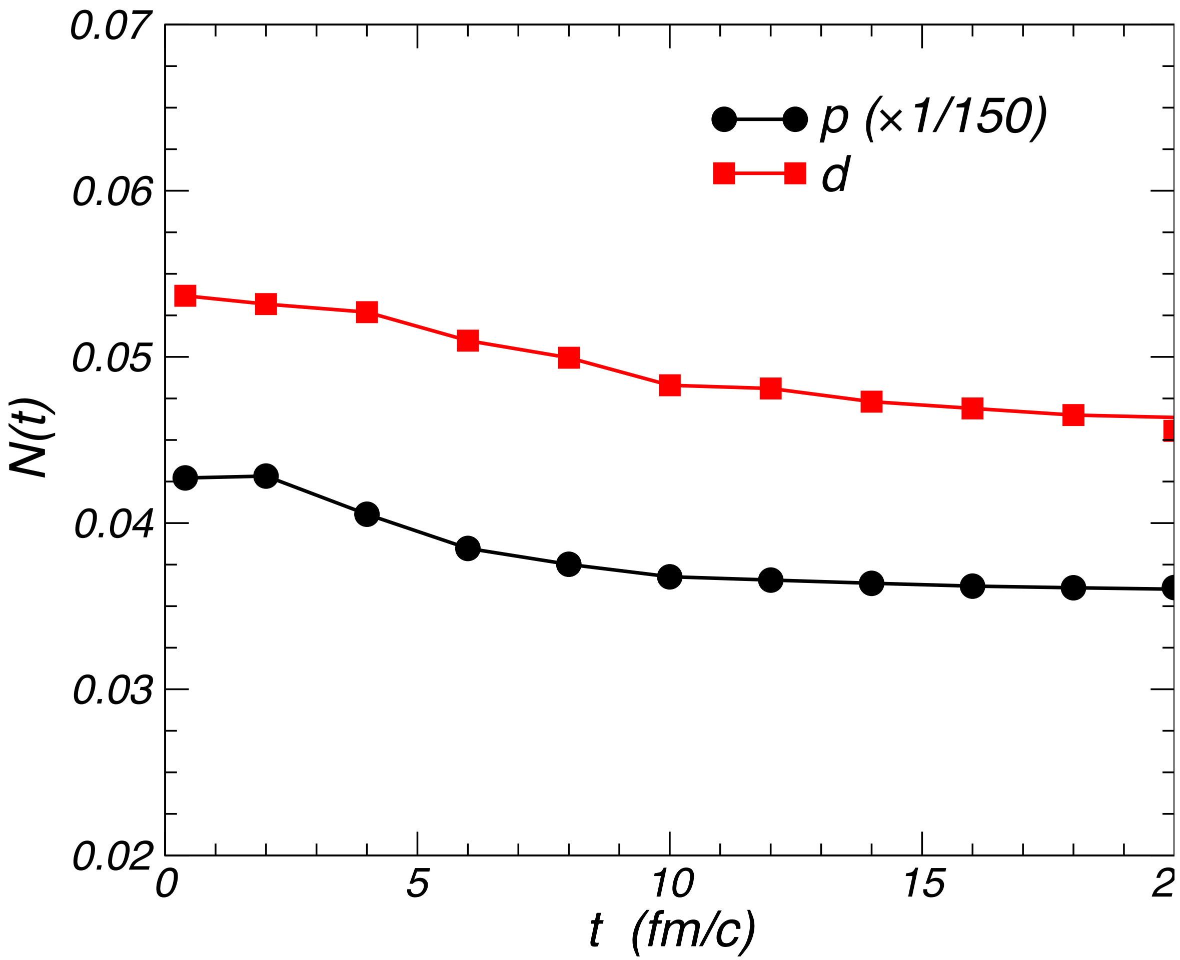

- Both proton and deuteron numbers decrease only slightly with time → early chemical equilibration

Deuteron production in kinetic theory

Cho & Lee, PRC 97, 024911 (2018)

$$\frac{dN_d(\tau)}{d\tau} = \sum_i \langle \sigma_{Ni} v_{Ni} \rangle n_i N_N(\tau) - \sum_i \langle \sigma_{di} v_{di} \rangle n_i N_d(\tau)$$

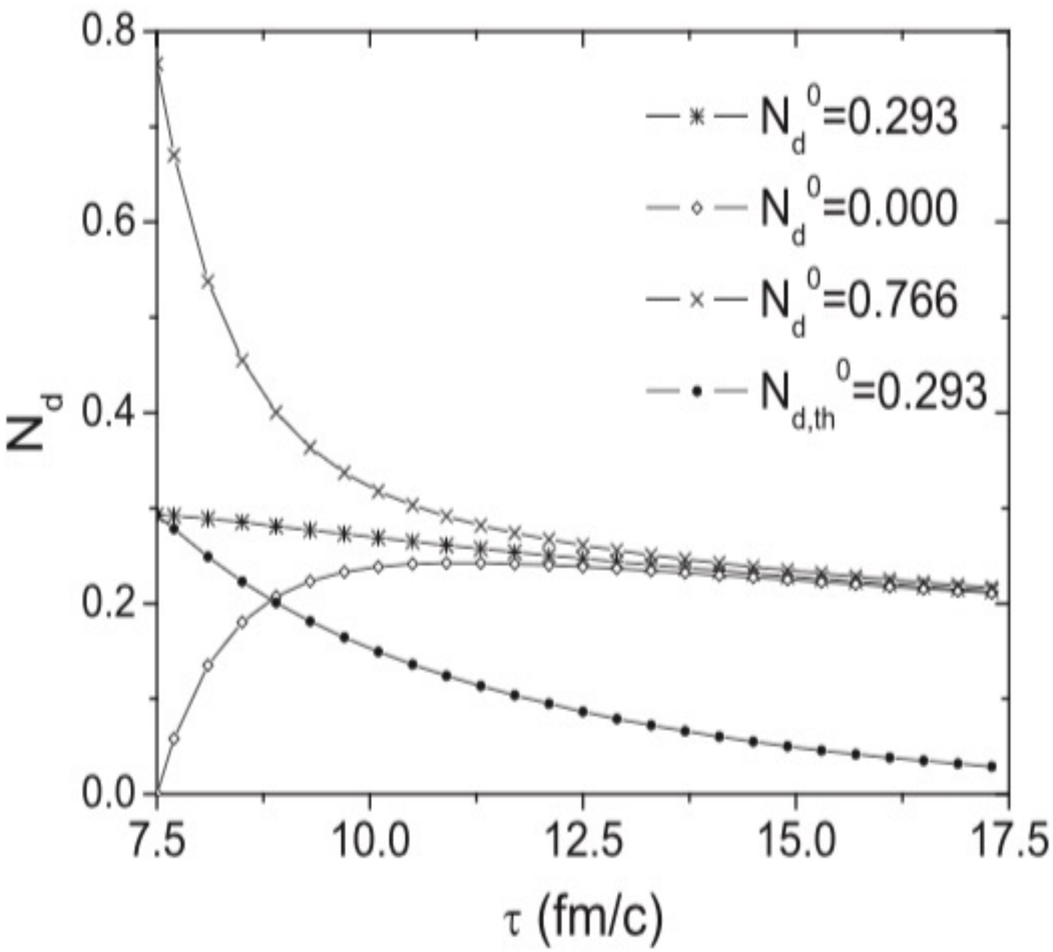

- Using

  $\sigma(d\pi^+ \to pp) = 50$ mb

  to take into account the large cross section due to $d\pi^+ \to pn\pi^+$
- Time evolution of temperature and volume from a schematic hydro model.
- Final abundance independent of initial abundance.

Nucleosynthesis in HIC via the Saha equation

Vovchenko, Gallmeister, Schaffner-Bielich & Greiner, PLB 800, 135131 (2020)

- Light nuclei are in chemical equilibrium: $\mu_A = \sum_i \mu_{A_i}$

$$N_A(T) = \frac{d_A m_A^2 T}{2\pi^2} K_2(m_A/T)\, e^{\mu_A/T}\, V \quad \rightarrow \quad \frac{N_A(T)}{N_A(T_{\rm ch})} \simeq \left(\frac{T}{T_{\rm ch}}\right)^{\frac{3}{2}(A-1)} \exp\left[B_A\left(\frac{1}{T} - \frac{1}{T_{\rm ch}}\right)\right].$$

- Thermal model: $\left[\frac{N_A(T)}{N_A(T_{\rm ch})}\right]_{\rm eq.} \simeq \left(\frac{T}{T_{\rm ch}}\right)^{-\frac{3}{2}} \exp\left[-m_A\left(\frac{1}{T} - \frac{1}{T_{\rm ch}}\right)\right]$

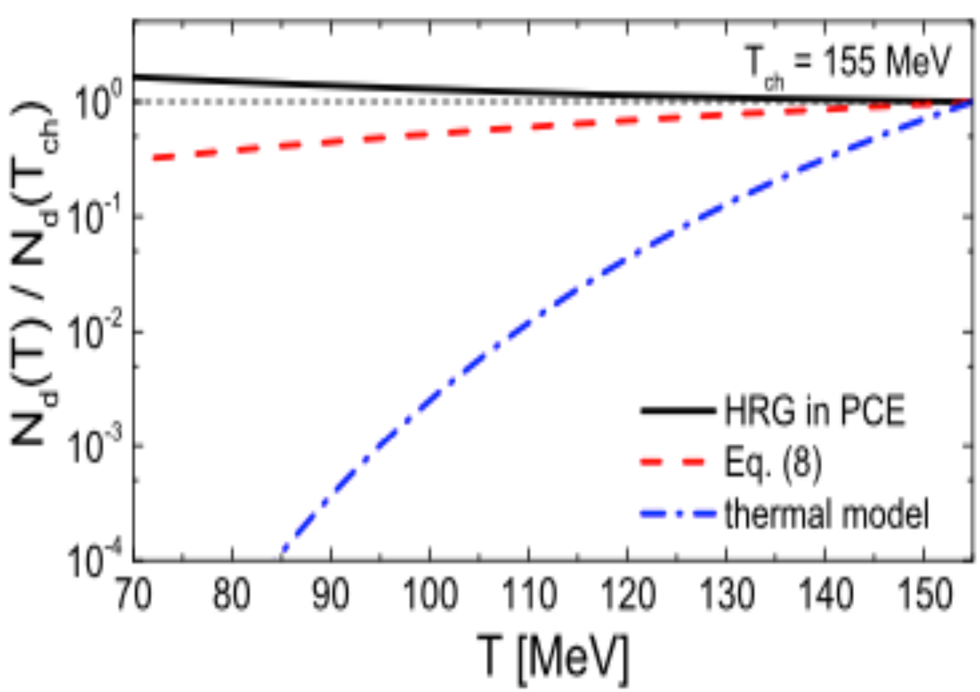

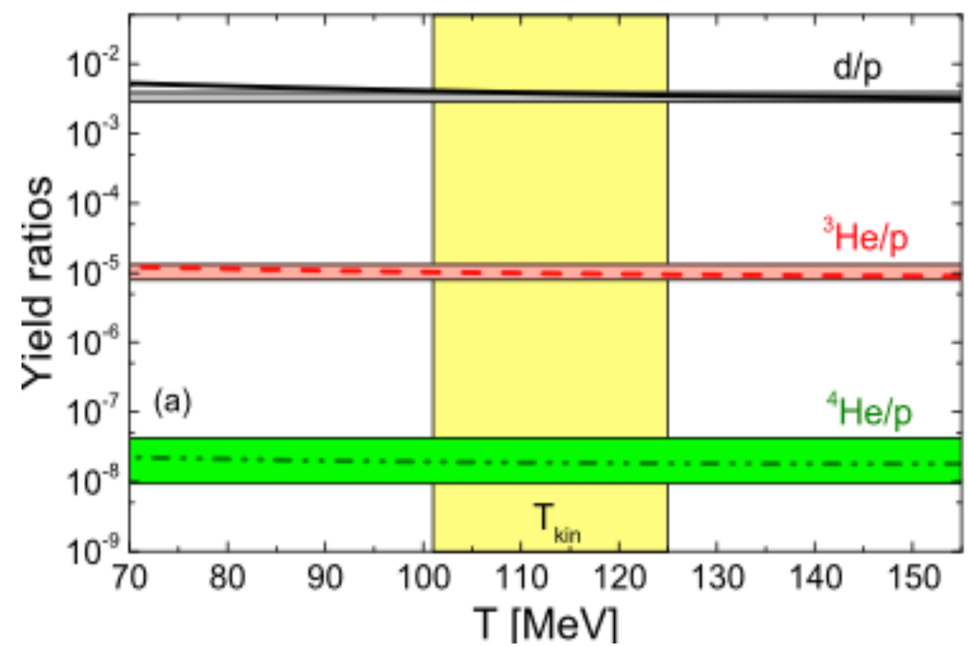

Deuteron production in SMASH

Oliinychekov, Pang, Elfner & Koch, PRC 99, 044907 (2019)

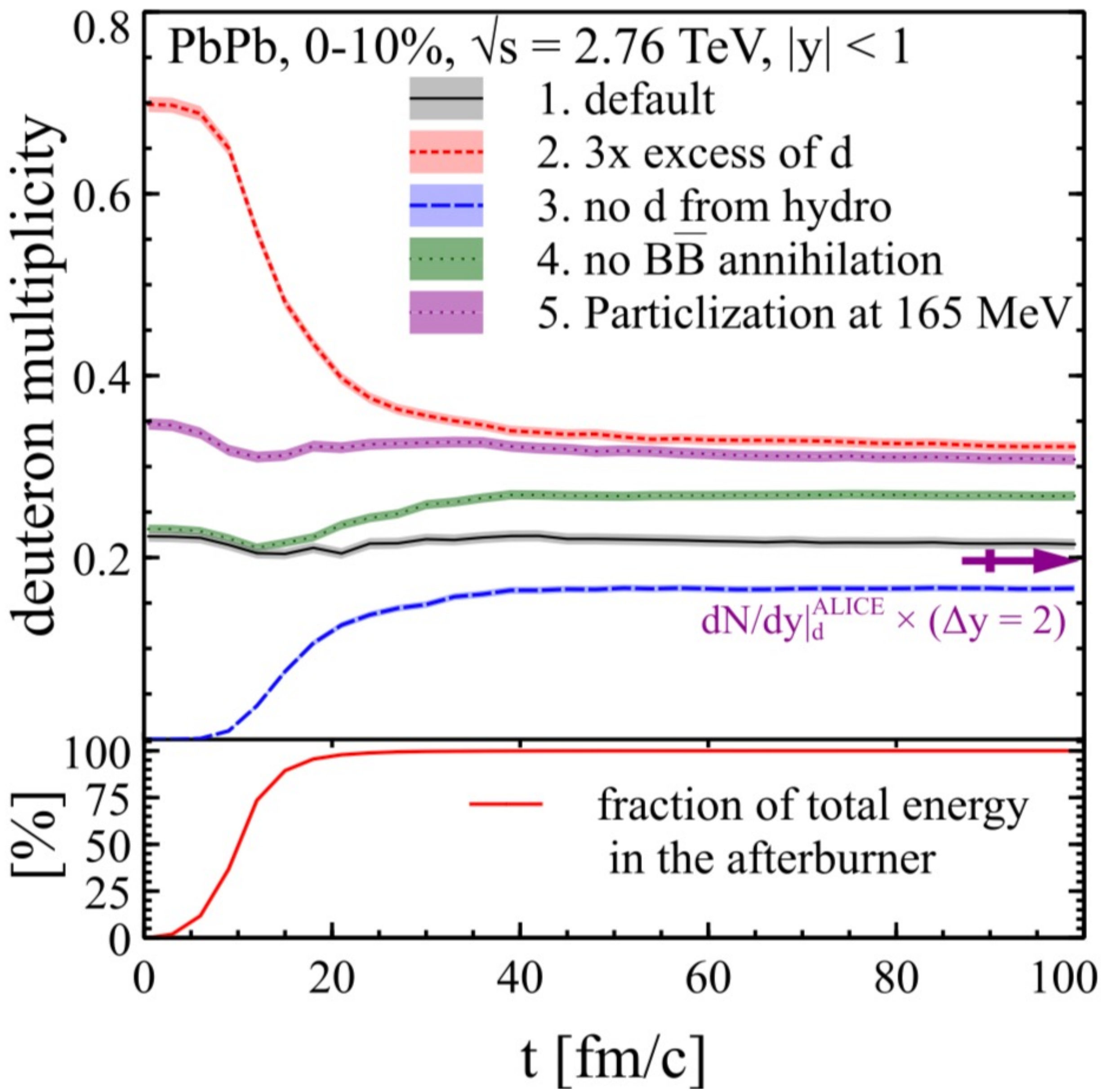

- Using a large $\pi NN \leftrightarrow \pi d$ cross section of about 100 mb.
- Deuteron number essentially remains unchanged during hadronic evolution

Light nuclei production from non-local many-body scattering

Sun, Wang, Ko, Ma & Shen, arXiv:2106.12742 [nucl-th]

$$\frac{\partial f_d}{\partial t} + \frac{\mathbf{P}}{E_d}\cdot\frac{\partial f_d}{\partial \mathbf{R}} = \frac{1}{2g_dE_d}\int\prod_{i=1}^{3}\frac{\mathrm{d}^3\mathbf{p}_i}{(2\pi)^3 2E_i}\frac{\mathrm{d}^3\mathbf{p}_\pi}{(2\pi)^3 2E_\pi}\frac{E_d\mathrm{d}^3\mathbf{r}}{m_d}2m_dW_d(\tilde{\mathbf{r}},\tilde{\mathbf{p}})$$

$$\left(\overline{|\mathcal{M}_{\pi^+n\to\pi^+n}|^2} + n\leftrightarrow p\right)\left[-g_\pi f_\pi g_d f_d\prod_i^3(1\pm f_i) + \frac{3}{4}(1+f_\pi)(1+f_d)\prod_{i=1}^3 g_i f_i\right]$$

$$\times(2\pi)^4\delta^4(p_1+p_2+p_3-p_\pi-p_d) \to \text{Good description of data}$$

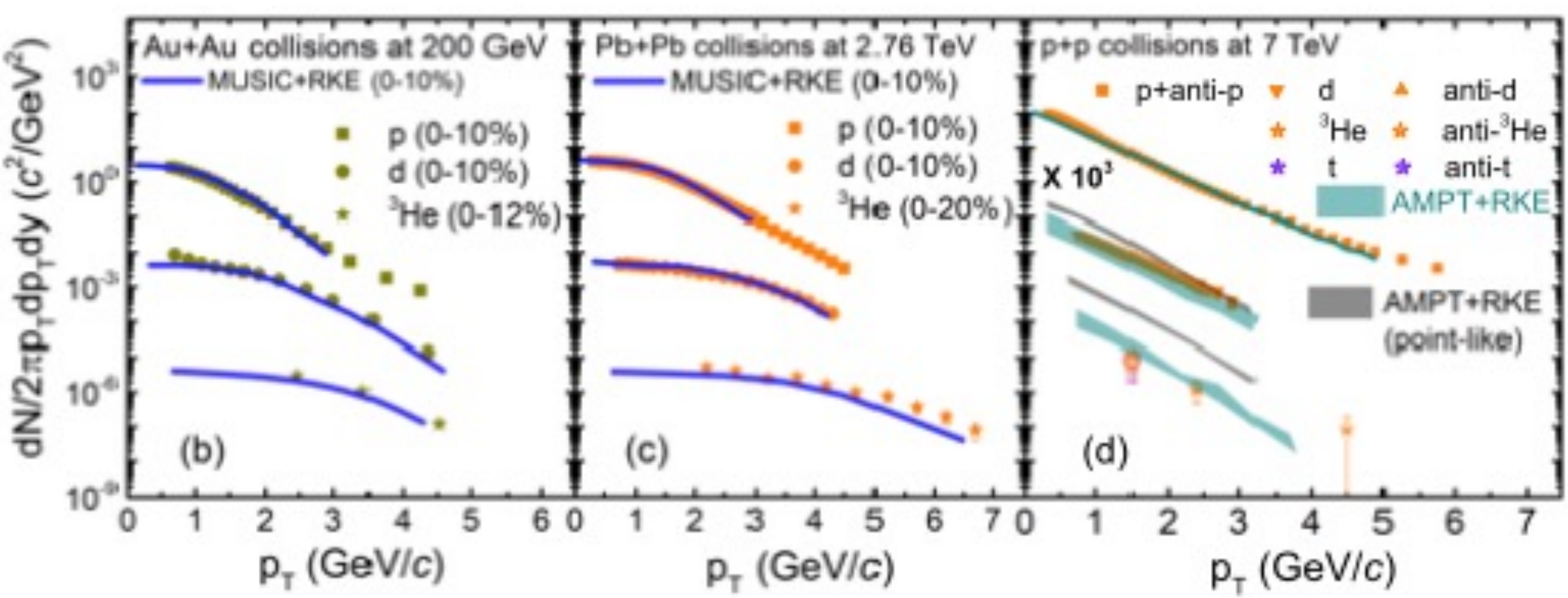

Hadronic rescattering effects on light nuclei production

Sun et al., arXiv:2207.12532 [nucl-th]

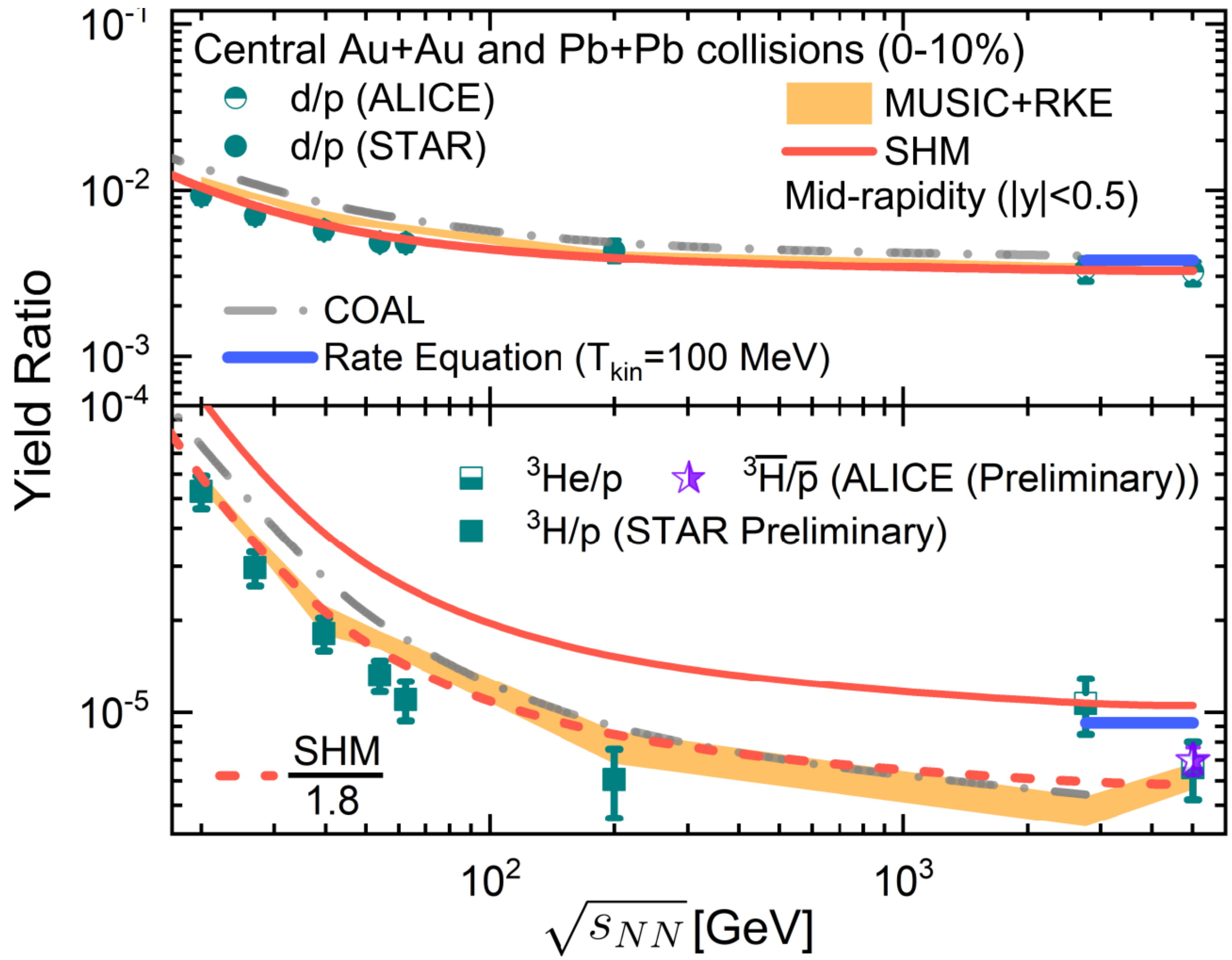

- *d/p* and *t/p* ratios are similar in kinetic approach and coalescence model.
- Hadronic re-scatterings reduce the triton yields by about a factor of 2 as a result of constant $tp/d^2 = 1/2\sqrt{3}$ and decreasing d/p due to decay of baryon resonances as the hadronic matter expands and cools.

Binding energies of light nuclei in hot nuclear matter

Typel, Roepke, Klahn, Blaschke & Wolter, PRC 81, 015803 (2010)

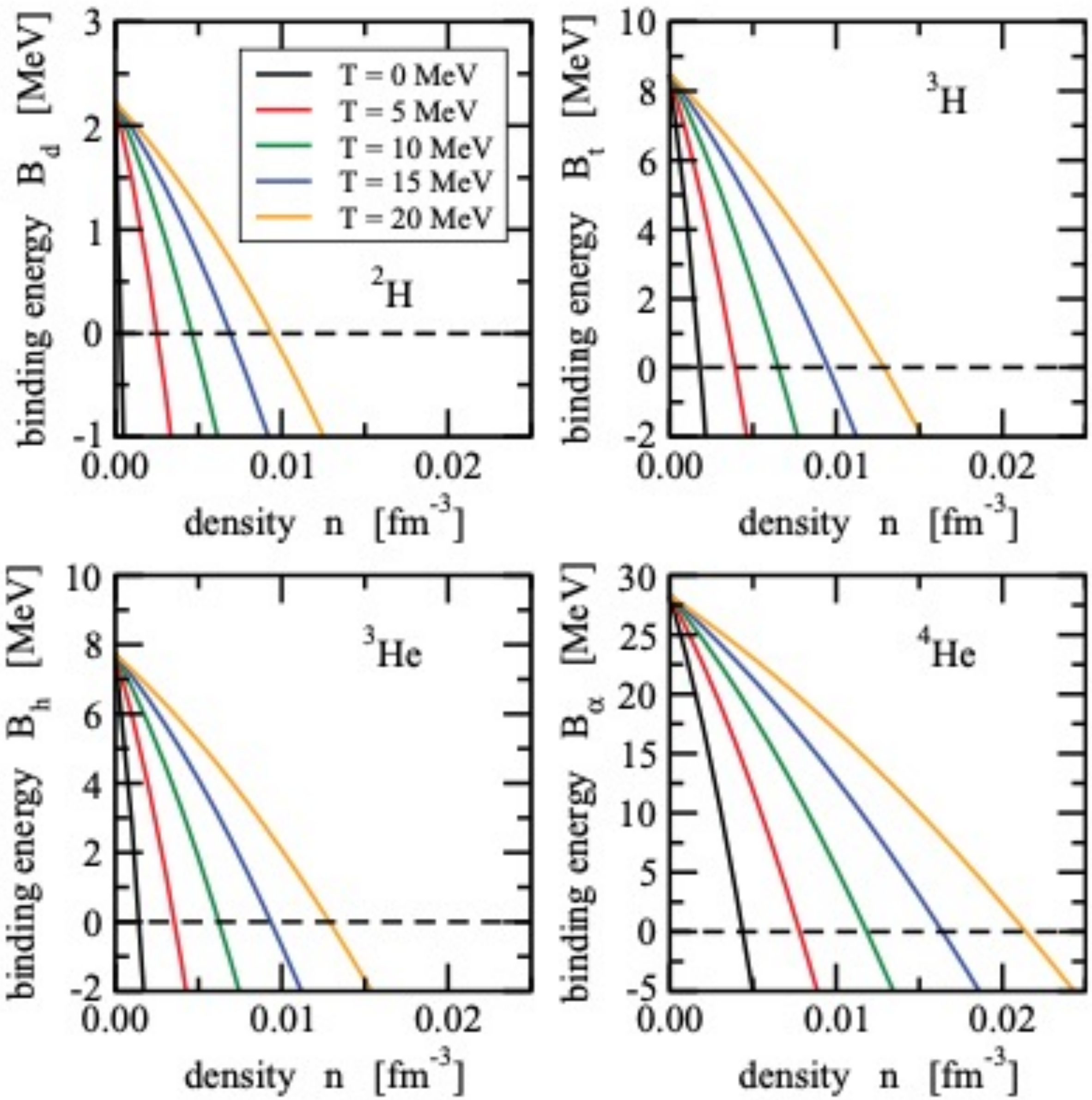

- Microscopic quantum statistical approach with relativistic mean-field model.
- Mott effect due to Pauli blocking can lead to bound light nuclei in denser nuclear matter as temperature increases.
- Are light nuclei bounded in hot pion gas?

Light nuclei production in intermediate-energy HIC

Rui Wang et al., in preparation

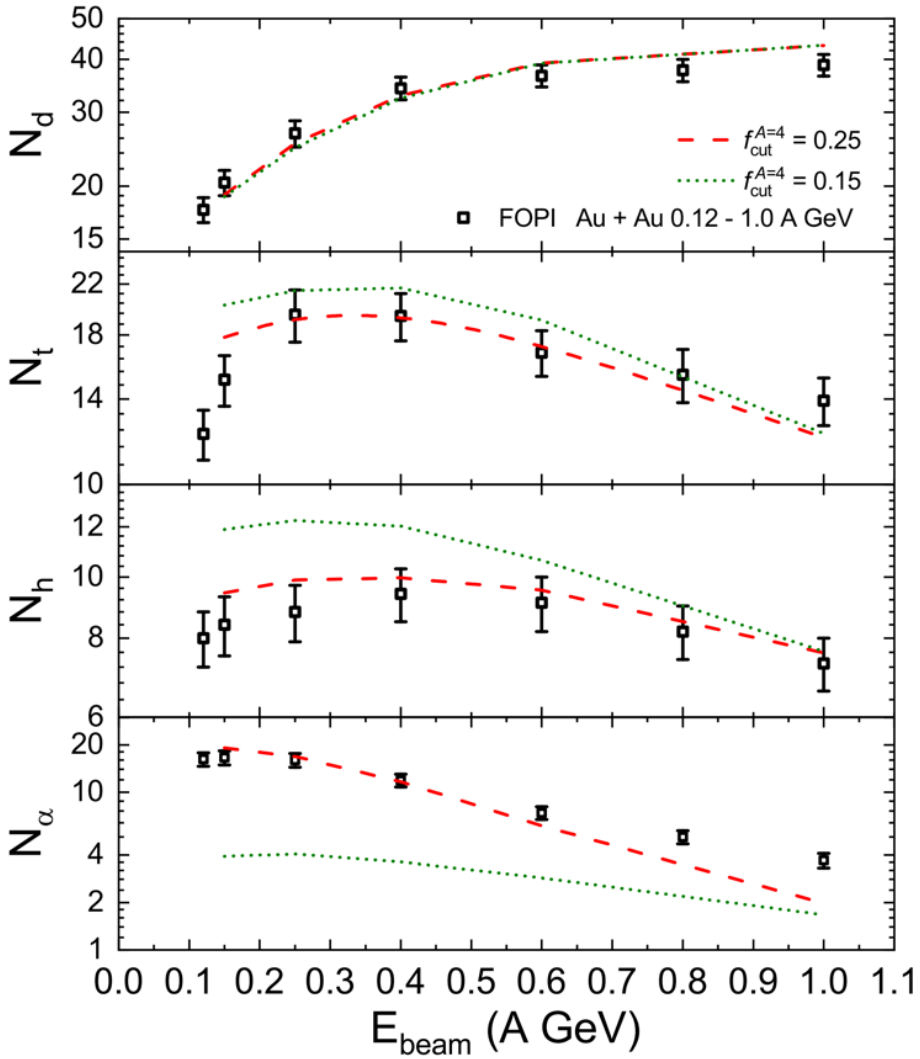

- Overlap of momentum distribution of constituent nucleons in nucleus A with that of nucleons in nuclear medium

$$\langle f_N \rangle^A \equiv \int f_N\left(\frac{\vec{P}}{A} + \vec{k}\right)\rho^A(\vec{k})\mathrm{d}\vec{k} \leqslant f_{\mathrm{cut}}^A$$

- The cut $f_{cut}^{A=2} = 0.11$, $f_{cut}^{A=3} = 0.16$, and $f_{cut}^{A=4} = 0.25$ reasonably reproduce the FOPI data in a wide range of E_{beam}.

Summary

- Light nuclei production may probe EoS and phase diagram of QCD matter.
- Nucleon density fluctuations enhance the production of light nuclei, providing a possible explanation for the experimental observations at SPS and RHIC.
- Coalescence model gives similar light nuclei yields in HIC as the thermal model if their binding energies are small compared to the temperature of the hadronic matter and the nucleon thermal wave length is much smaller than their sizes. Both results are similar to that from transport model studies in which deuterons are assumed to remain bounded and can be produced and dissociated.
- Kinetic approach with light nuclei finite size effect can naturally explain the suppressed production of light nuclei in collisions of small systems.
- Light nuclei produced in intermediate-energy HIC can probe their in-medium properties.